

# Design and Production of Thin-Walled UHPFRC Footbridge

P. Tej, P. Kněž, M. Blank

**Abstract**—The paper presents design and production of thin-walled U-profile footbridge made of UHPFRC. The main structure of the bridge is one prefabricated shell structure made of UHPFRC with dispersed steel fibers without any conventional reinforcement. The span of the bridge structure is 10 m and the clear width of 1.5 m. The thickness of the UHPFRC shell structure oscillated in an interval of 30-45 mm. Several calculations were made during the bridge design and compared with the experiments. For the purpose of verifying the calculations, a segment of 1.5 m was first produced, followed by the whole footbridge for testing. After the load tests were done, the design was optimized to cast the final footbridge.

**Keywords**—Footbridge, UHPFRC, non-linear analysis, shell structure.

## I. INTRODUCTION

THE bridge serves as a pedestrian bridge and has a span of 10 m. The bridge is designed with double curvature in the vertical and transverse direction with a camber of 0.4 m. The cross section of the bridge has a width of 1.5 m, and it is U-shaped. The bridge deck consists of a bottom plate with only 45 mm thickness and 30 mm thick side desks which serve as railings. Railing height is 1.1 m in the middle of bridge span and 1.5 m in the support area. The bridge has no conventional reinforcement and is only reinforced by steel dispersed fibers. Production of footbridge is detailly presented in [10].

The bridge is made of ultra-high performance fibre reinforced concrete (UHPFRC). The main outstanding features of this material include the high compressive strength (120-180 MPa) and the high tensile bending strength (20-40 MPa) [1]-[4]. High levels of strength are provided by using steel fibers. They absorb energy and control cracks growth until failure [5]-[7]. High water impermeability is provided by a dense cement matrix and a very low level of porosity with unconnected pores. It is caused by a very low water-cement coefficient, close packing of fine grains of solid particles and by reaction of a very fine reactive material admixtures (microsilica, slag and fly ash) [1]. From high water impermeability, high resistance to frost and high durability are derived [2].

## II. COMPUTER ANALYSIS

Bridge model was created and calculated in a software ATENA 3D [8], [9]. The model is divided into 0.5 m wide

parts where deck and railings are modeled as iso-shell macro elements (bottom plate and two railings) bonded with small standard macro-elements, which are structured to simulate the curvature of the bridge. Anchoring deck areas are also made as standard macro-elements. These macro elements have specified material item 3D Nonlinear Cementitious2 with parameters of UHPFRC class C110/130. The tensile strength of concrete is considered as a value of 9.5 MPa according to experiments. Calculation is performed as a basis for the experiment, material properties was not reduced by material coefficients.

The bridge is supported by the distributing macro-elements, whose lower surface is divided by the line on which are applied such conditions that simulate fixed joint at one end and movable at the other end. Loading the bridge is except the load of the railings on the lateral force via the surface load applied to the appropriate areas of individual macro-elements forming the bridge structure. The bottom plate of the bridge was loaded on whole surface by load of  $4.2 \text{ kN/m}^2$ , and subsequently up to structural failure, further part with the greatest eccentricity to cause torque to structural failure. Railing was loaded with a force corresponding to  $1 \text{ kN/m}$  at the top edge and vertical force until failure of the whole structure. The whole bridge was also loaded by temperature change of  $+40^\circ\text{C}$  and  $-35^\circ\text{C}$ .

The model was meshed by quadratic brick elements with a base edge length of 0.25 meters for Isoshell macro elements. Standard macro elements are meshed by tetra elements with edge length reduced to 40% of base edge length for anchoring and supporting elements and to 20% of base edge length for elements that bond deck and railings together.

As seen in Fig. 4, the bearing capacity of the construction achieves satisfactory values ( $16.9 \text{ kN/m}^2$ ), which are well above the required load capacity ( $4.2 \text{ kN/m}^2$ ), despite its subtlety.

## III. PRODUCTION OF FOOTBRIDGE

### A. Test of Casting on the Footbridge Section

One of the main problems for the production of a shape-complex bridge is casting technology. Especially thanks to the double curvature and the very thin walls of the footbridge, it was decided to cast the footbridge "upside down". Due to the relatively complicated and extremely unusual thin-wall construction of the footbridge for cementitious materials, it was decided to produce a test sample of footbridge. Control casting was carried out on a section of a footbridge of 1.5 m length. The main objective was to verify the casting process itself, the resulting state of the surface of the element, to verify

Petr Tej is head and Petr Kněž and Marek Blank are Ph.D. students of Department of Structural Engineering at Klokner Institute, Czech Technical University in Prague, Czech Republic (e-mail: petr.tej@cvut.cz, petr.knez@cvut.cz, marek.blank@cvut.cz).

the correct consistency of the fresh UHPFRC mixture and the mold's ability to withstand the pressures of fresh concrete. A very important parameter was also the monitoring of the solidification process and the possibility of removal the formwork to reduce the risks associated with volume changes. The formwork was wooden with laminated surfaces. Formwork has to be designed to withstand the fresh concrete pressure, which is due to the high fluidity of the fresh mixture

main load when casting. In order to obtain a curved shape during the casting upside down, it meant that all the surfaces would be enclosed in formwork. It was therefore necessary to examine the potential problems with the surfaces of the structure enclosed in the formwork as the assumption for the casting of the entire platform was to have only two filling holes.

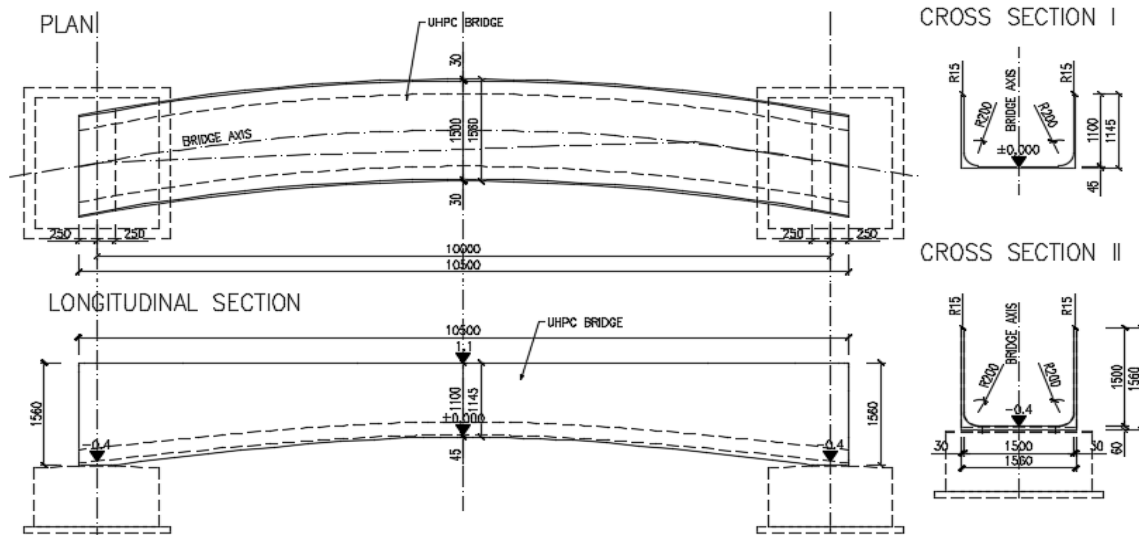


Fig. 1 Plan, longitudinal and cross section of the final footbridge

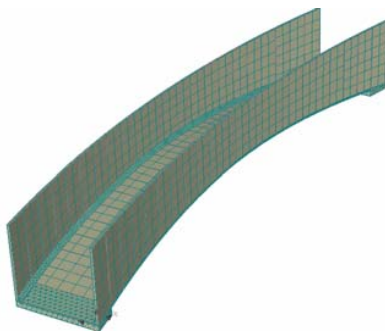


Fig. 2 Finite element mesh

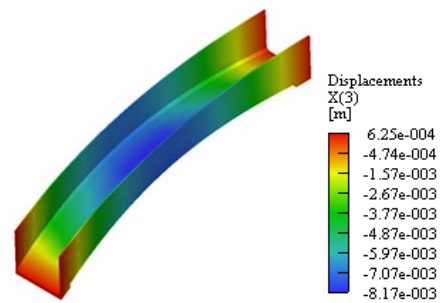


Fig. 4 Vertical deflection of the structure before failure, the applied force of 16.9 kN/m<sup>2</sup>, the maximum deflection value -8.17 mm



Fig. 3 Segmentation of macroelements to surfaces

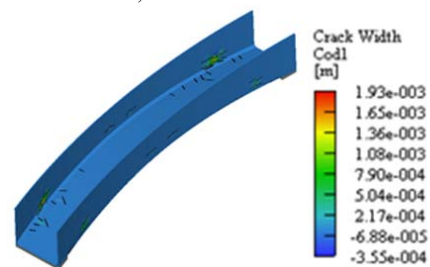


Fig. 5 Cracks for the structure before failure, the applied force of 16.9 kN/m<sup>2</sup>, the maximum crack width 1.93 mm

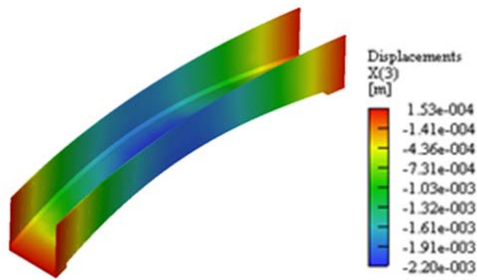


Fig. 6 Vertical deflection of the structure before failure, the applied force of  $4.2 \text{ kN/m}^2$ , the maximum deflection value  $-2.2 \text{ mm}$

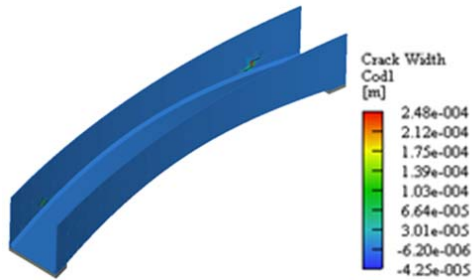


Fig. 7 Cracks for the structure before failure, the applied force of  $4.2 \text{ kN/m}^2$ , the maximum crack width  $0.248 \text{ mm}$

Control casting showed:

- It has been demonstrated that it is possible to completely fill the form without caves and macropores,
- Smooth and very aesthetically acceptable surfaces have been created on visible and concealed surfaces,
- The bottom surface of the structure enclosed in the formwork showed an assumed increased pore frequency, yet the surface was homogeneous and aesthetically very acceptable.

#### B. Optimizing the UHPFRC Recipe

The UHPFRC mixture was optimized. The final mixture consists of cement CEM II 52.5 N, fine aggregate with a maximum size of  $2 \text{ mm}$ , slag, microsilica and steel microfiber

with a length of  $13 \text{ mm}$ . The bulk density of the fibers was chosen for this application of  $1.5\%$ . The volume of water and superplasticizer has been optimized with regard to workability. This was checked for each mixer by spilling the Hagermann cone. The tested optimal spill value was determined at  $310 \text{ mm}$ . Optimization of the recipe during the production of the footbridge test segment included not only the setting of workability but also the determination of the mechanical properties of the material over time. The first tests were carried out 5 hours after casting.



Fig. 8 Formwork of test sample



Fig. 9 Sample after removal of mold

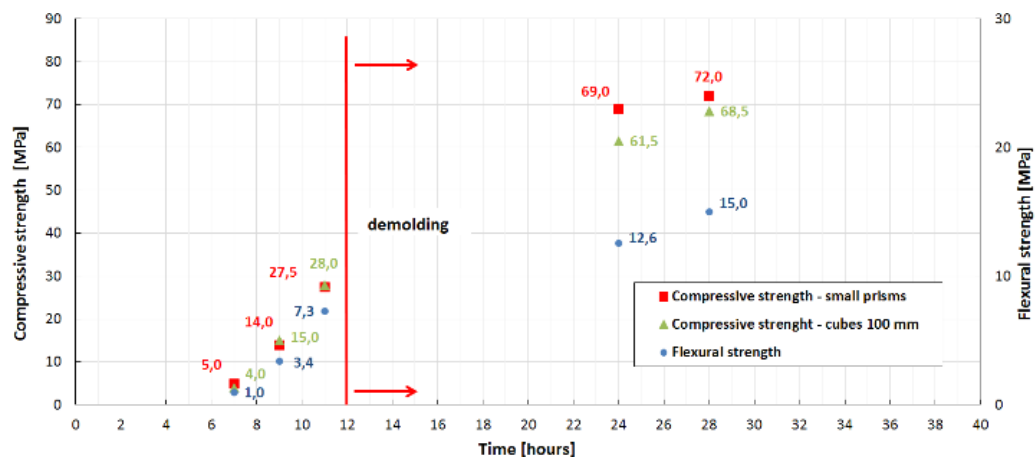


Fig. 10 Development of mechanical parameters of UHPFRC within 40 hours after casting

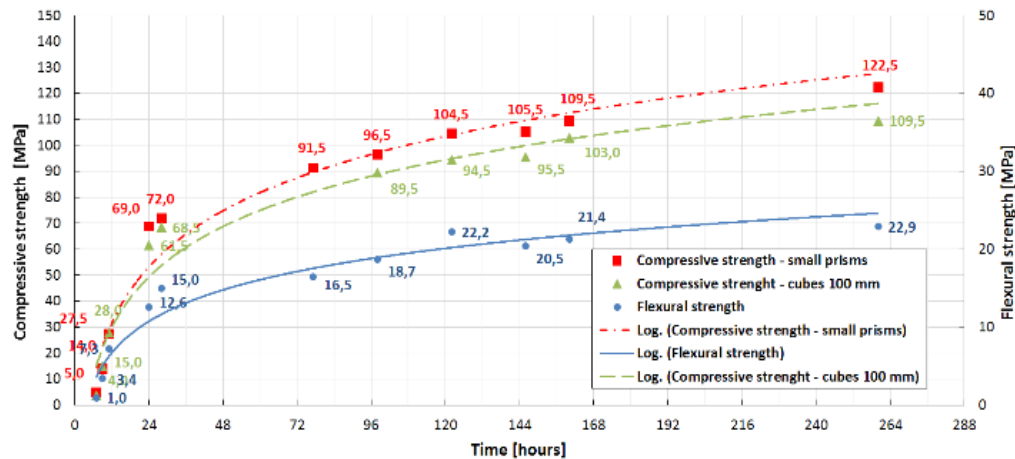


Fig. 11 Development of compressive and flexural strength at first 10 days after casting

Another set of samples was tested for 2 hours and the tests continued until the test element was removed from the mold. The development of material properties up to 40 hours after casting is shown in Fig. 10. The decisive compressive strength for demolding was set at 30 MPa.

#### C. Formwork Production

Based on the successfully completed control footbridge sample, a final formwork of the entire footbridge was designed and prepared to achieve the desired double curve of the footbridge.



Fig. 12 Wooden formwork of footbridge I

Only two holes for pouring UHPFRC at the ends of the footbridge bearing area were prepared. A very complicated formwork construction has to be optimized for quick and easy release and removal of the element from mold. The reason was to minimize the risk of volume changes to crack formation. The formwork was sufficiently reinforced with a wooden beam system to withstand fresh concrete.



Fig. 13 Removing of wooden formwork

#### D. Casting of the Footbridge I

The prepared mold was filled in January. The footbridge was casted at low temperatures in the winter. The temperature of the raw materials was between 1 and 8 °C. The final volume of the UHPFRC mixture was 1.4 m<sup>3</sup>. A total of three batches were mixed. These were successively liths from the two outer openings in the area of supports. The consistency of fresh concrete was verified by spreading a small Hagermann cone prior to the start of mold filling. The cold environment had a positive effect on the consistency and the beginning of the solidification. There was no problem with working joints between doses. No vibrators were used when storing and compacting itself. The self-extinguishing behavior of the mixture was used. Due to the low temperature in the hall, the mold was insulated with polystyrene boards, overlapped by foil and portable thermometers were used after the casting ended. The maximum temperature outside mold did not reach 40 °C. Casting the whole element took approximately one hour. At the same time, the compression and flexural strength development was determined to determine the demolding time. The moment of release of formwork was set at 11-12 hours after casting. The additional heating took place for the next 5 days. After 4 days, the temperature of the UHPFRC and the environment was equalized. All surfaces of the thin plates including the top surface of the bridge were very smooth and of very good quality. The material completely filled the entire thin-walled formwork structure without any problems. The footbridge was exported from the hall to a storage site outside the hall, 7 days after casting. The element was transported by crane and placed on polystyrene boards to allow volume changes.

The resulting mechanical parameters of UHPFRC after 28 days were:

- Compressive strength on cubes 100 mm - 150 MPa
- Flexural strength on beams 40x40x160 mm - 22.6 MPa
- Elastic modulus on cylinders 150x300 mm – 51 GPa

#### E. Handling and Static Loading Test of Footbridge I

After reaching the age appropriate for turning the footbridge

into the final position, the footbridge was exported to the open air and turned by two cranes in a vertical position. This operation required very strict safety conditions. By manipulating with the footbridge in the vertical position, the tensile cross-sectional strength was verified - the creation of additional cracks from the handling was not monitored on the footbridge. The footbridge was placed on rubber washers and turned to reinforced concrete panels so that a load test can be performed.

The loading test was carried out by placing sandbags on the footbridge in successive loading steps. During the test, the deflection of the footbridge was measured in the middle of the span, and the vertical wall deflection was also measured in the middle of the span. During the last loading step, the plate was damaged by a deflection of the outer wall at the point of transition of the board into the vertical railing. This was due to the overall lower stiffness of the structure than was assumed in the model. In individual steps, a higher deflection was measured, which resulted in the railing to be lifted and the longitudinal crack at the point of rise. The load would be increased until breakdown of the footbridge for the validation of the calculation models.



Fig. 14 Rotation of footbridge I



Fig. 15 Perform static loading test on footbridge I

#### *F. Conclusions from Footbridge I Test*

Material properties of the UHPFRC, the design of the formwork, and the casting technology of the footbridge allow the manufacture a complex thin-walled double-arched footbridge. The footbridge is stable and well manipulated after hardening. Several lessons have been learned from the production technology about the ideal time of demolding, the rise of strength, and the effect of curvature on microcracks on its surface. A static load test has shown that the rigidity of the railing walls and their connection to the bridge walls do not meet the model's prerequisites and it is necessary to adjust the footbridge shape by reinforcing the railing walls to a 35-mm radius of curvature at the corner.

All of these findings have been carefully researched and incorporated into the design of the final footbridge, formwork production and the final casting technology process so that the final footbridge is produced in the highest possible quality. This footbridge is now used for surface treatment tests where coatings are applied to the UHPC surface, the surface is buffed, and further tests of long-term character are carried out. These tests are intended to extend the knowledge of the behavior of the material and, in particular, surfaces exposed to normal weather conditions.

#### *G. Casting of the Footbridge II*

Casting of the final footbridge was in May. Due to the relatively favorable conditions on the hall, the formwork was not required heat up before or after the casting. Casting took place in the early hours, so the air temperature correlated with the gradual development of temperatures during the hydration of concrete. These values were compared with the data obtained during casting of the footbridge I., where the temperature development was monitored very complexly. The rise of the strengths was controlled by regular tests of the accompanying specimens, as well as the development of the temperature of the concrete. The demolding procedure included a very complex sequence of operations, and then, the footbridge was transported to the area in front of the operating hall. After about 2 months of outdoor treatment, a static loading test was performed. The test confirmed the correctness of the modification, the design accuracy, and the load capacity of the footbridge.



Fig. 16 Formwork of footbridge II



The resulting mechanical parameters of UPCFRC after 28 days were:

- Compressive strength on cubes 100 mm - 144 MPa
- Flexural strength on beams 40x40x160 mm - 28.3 MPa
- Elastic modulus on cylinders 150x300 mm – 49.8 GPa

#### *H. Handling and Static Loading Test of Footbridge II*

A horizontal rotation method was chosen to rotate the final footbridge, a so-called "chicken-on-rooster" method. After reaching the necessary age of the footbridge, the internal space was reinforced with wooden frames, and the whole structure was reinforced with wooden stiffening. At the center of gravity of the cross section, a steel tube extending through the entire length of the footbridge was designed. At the end of the tube, the footbridge was lifted and turned around its axis. This procedure was complicated due to the change of the center of gravity position along the length of the footbridge due to double curvature. However, the rotation operation was accomplished, and the final footbridge was exported to the open area and stored on rubber washers.

The loading test was carried out by placing sandbags on the footbridge in successive loading steps. During the test, the deflection of the footbridge was measured in the middle of the span and the vertical wall deflection was also measured in the middle of the span. The footbridge was loaded until the standard load had been reached. During the load test, the footbridge acted according to the assumptions set out in the numerical analysis. There were no excessive deformations or cracks of larger widths. The load to breakdown of the footbridge is not continued - the produced footbridge will be used for long-term testing under normal operation.



Fig. 17 Rotation of footbridge II



Fig. 18 Rotation of footbridge II



Fig. 19 Perform static loading test on footbridge II

#### IV. COMPARISON OF FOOTBRIDGE I AND FOOTBRIDGE II

As can be seen from the figures, geometrical modifications were made in the manufacture of the footbridge II. In order to achieve better static behavior of the structure, the ramp radii in the wall-plate contact were increased first. This creates longitudinal supporting ribs, which significantly strengthen the structure. Further, the thickness of the plate was 45 mm in the center, which gradually passes to 60 mm at the end cross members. Comparison of geometry is shown in Figs. 20 and 21.



Fig. 20 Footbridge I



Fig. 21 Footbridge II

#### V. SURFACE FINISHES

A number of procedures have been prepared and tried to

finalize the surfaces. First, the entire structure was sprayed with pressurized water and stripped of production impurities. This was followed by brushing the whole surface with a hand-held grinder with copper wires. This modification is shown in Fig. 22.



Fig. 22 Surface after brushing

As can be seen, brushing will result in the unification of the entire surface and the inversion of small shrinking cracks. The final coating will etch the surface of the bobbin with acid. Different types of acids react with the substrate and create a different surface color. In Fig. 23, there are three strips treated with three types of acids. The resulting surface will be treated as a medium, reddish-brown strip.



Fig. 23 Surface after acid treatment

## VI. CONCLUSION

The paper presents the design and production of the footbridge made of ultra-high performance concrete. The bridge deck consists of a bottom plate with 45 mm thickness and 30 mm thick side desks which serve as railings.

The shape of the footbridge was based on the requirement to pass at least the standard load on this type of construction ( $4.2 \text{ kN/m}^2$ ) while maintaining the maximum possible subtlety of the structure without the need to insert the conventional reinforcement made possible by using UHPFRC concrete.

By calculation, it was shown that the load bearing capacity of the structure has a value of  $16.9 \text{ kN/m}^2$  of continuous planar load which are well above the required load capacity ( $4.2 \text{ kN/m}^2$ ), despite the subtlety of the construction. The design

methods and the load-bearing capacity of the footbridge were verified and confirmed by loading tests.

Currently, finishing of the footbridge surfaces is being carried out in order to fulfill all the operational and aesthetic properties. Subsequently, the footbridge will be placed on prepared foundations and put into the test operation for long-term monitoring.



Fig. 24 Final visage of footbridge II



Fig. 25 Final visage of footbridge II



Fig. 26 Final visage of footbridge II

## ACKNOWLEDGMENT

Theoretical basis for the presented results were obtained under the support of the research project TH02020730 of the Technology Agency of the Czech Republic and by the Czech Technical University in Prague, projects SGS18/165/OHK1/2T/31 and SGS17/161/OHK1/2T/31.

## REFERENCES

- [1] C. Shi, Z. Wu, J. Xiao, D. Wang, Z. Huang and Z. Fang, "Review on ultra high performance concrete: Part I. Raw materials and mixture design," *Construction and Building Materials* 101, p. 741-751, 2015.
- [2] D. Wang, C. Shi, Z. Wu, J. Xiao, Z. Huang and Z. Fang, "Review on ultra high performance concrete: Part II. Hydration, microstructure and properties," *Construction and Building Materials* 96, p. 368-377, 2015.
- [3] Proceedings of the 2nd International symposium on UHPC, Kassel, March 5-7, 2008.
- [4] Proceedings from HIPERMAT 3rd International symposium on UHPC and Nanotechnology for High Performance Material, Kassel, March 7-9, 2012.
- [5] JSCE-USC, *Recommendations for Design and Construction of Ultra-High Strength Fiber-Reinforced Concrete Structures – Draft*.
- [6] AFGC/SETRA, *Ultra High Performance Fibre-Reinforced Composites, Recommendations*. Paris CEDEX, 2013.
- [7] J. Kolísko, M. Rydval and P. Huňka, "UHPC – Assessing the Distribution of the Steel Fibre and Homogeneity of the Matrix." *fib Symposium Tel Aviv*, 2013.
- [8] V. Červenka, J. Červenka and R. Pukl, *ATENA – A tool for engineering analysis of fracture in concrete*. Sadhana 27/4, 2002.
- [9] J. Červenka and V. K. Papanikolaou "Three Dimensional Combined Fracture-Plastic Material Model for Concrete." *Int. Journal of Plasticity* 24/12, 2008.
- [10] J. Kolísko, D. Čítek, P. Tej and M. Rydval, "Production of Footbridge with Double Curvature Made of UHPC." In: *Fibre Concrete 2017, Materials Science and Engineering*. vol. 246. ISSN 1757-899X.